



Research Article

Thermal behavior and evolved gas analysis for pyrolysis of olive pomace, coal, and their blends using TGA/FTIR

Hasan MERDUN^{1,*}, Balkis YAHYAOU¹

¹Department of Environmental Engineering, Akdeniz University, Faculty of Engineering, Antalya, 07058, Türkiye

ARTICLE INFO

Article history

Received: 29 September 2023

Revised: 16 January 2024

Accepted: 18 January 2024

Keywords:

Coal; Co-pyrolysis; Olive Pomace; Synergistic Effect; TGA/FTIR

ABSTRACT

This study analyzed the thermal behavior and evolved gas for pyrolysis of olive pomace (OP), coal, and their five blends at five different heating rates using TGA/FTIR. Furthermore, synergistic effects were investigated during the co-pyrolysis of OP and coal. Mass loss (ML) systematically increased in the second stage of all samples from pure coal toward pure OP, but the corresponding temperatures and temperature ranges decreased. The synergistic effect was observed for ML and maximum differential thermogravimetry (DTG_{max}) in the blends of 60% OP + 40% Coal and 80% OP + 20% Coal. The absorbances of CO and CO₂ were similar, but the absorbances of CH₄, NO_x, and SO₂ showed similar and clear trends with a single peak at temperatures of 200-600°C as in TG and DTG curves. The peak intensity and hence the contribution to CH₄, NO_x, and SO₂ emission increased as the OP content increased in the blend. The highest peak intensity with the largest contribution to CO emission was observed in the pure OP sample, whereas the lowest peak with the least contribution was observed in the 40% OP + 60% Coal sample. Similar behavior was observed in the CO₂ absorbance. The results of this study with different thermal behavior, synergistic effects, and gas emissions during pyrolysis of OP, coal, and their blends suggest conducting further studies under different experimental conditions to understand better and get useful knowledge for the design of industrial pyrolysis reactors.

Cite this article as: Merdun H, Yahyaoui B. Thermal behavior and evolved gas analysis for pyrolysis of olive pomace, coal, and their blends using TGA/FTIR. J Ther Eng 2025;11(1):112–126.

INTRODUCTION

Energy demand will considerably increase shortly due to the increase in the world population and industrialization of developing countries. Currently, energy is significantly supplied from fossil fuels such as oil, coal, and natural gas [1]. However, the depletion of fossil fuels and

greenhouse gas (GHG) emissions, which are responsible for global warming and climate change, from these fuels to the environment has encouraged researchers to develop alternative energy sources. Biomass takes attention as a possible option; where it is abundant, cheap, carbon-neutral, and renewable, and therefore, has great potential as an energy source [2, 3]. Biomass is defined as non-fossilized and

*Corresponding author.

*E-mail address: merdun07@gmail.com

This paper was recommended for publication in revised form by Editor-in-Chief Ahmet Selim Dalkılıç



biodegradable organic material sourced from plants, animals, and microorganisms. As one of the potential biomass sources olive pomace (OP), emerging from food waste and not competing with food production, has also great energy potential.

The OP, a by-product of the olive oil industry with the two-stage centrifugation system, is composed of water, oil, olive skin, olive pulp, and olive stone [4]. Among all biomass types, OP is a suitable feedstock in the Mediterranean Region Countries because Spain produces approximately 50% of the worldwide olive oil, and the other 50% is produced by Italy, Tunisia, Greece, and Türkiye, respectively [5]. These countries generate a large amount of seasonal waste as they can produce approximately 2500 kg of olives and 875 kg of OP from one hectare (ha) of olive tree planted area [6]. Türkiye's olive production alone in 2019 is 1 500 467 tons and the amount of waste generated is 345 771 tons [7]. Dried OP contains high amounts of organic matter, proteins, water-soluble fats, water-soluble carbohydrates, and water-soluble phenolic substances. It also has high potassium content and low phosphorus and micronutrients [2]. However, it is harmful to the environment because of its phytotoxicity and antimicrobial properties [8]. These adverse effects can be significantly reduced if OP is converted into energy and chemicals through thermochemical technologies [2, 9, 10]. Biomass can be converted into energy by biochemical or thermochemical technologies. Fermentation and anaerobic digestion produce ethanol and biogas as biochemical conversion, whereas thermochemical conversion includes combustion, pyrolysis, gasification, and liquefaction [11]. Since OP has low biodegradability and a high organic matter content, pyrolysis of OP has several advantages over conventional biochemical processes as it decreases the process costs by producing valuable products applied to various fields [12]. Pyrolysis is a commercialized technology for the complete conversion of OP into biofuels.

Pyrolysis is the decomposition of organic material/biomass into solid (biochar), liquid (bio-oil), and gas (mixture of gases) products by externally supplying heat under an inert atmosphere. The distribution of products depends on biomass types and characteristics and pyrolysis operation parameters such as temperature, heating rate, carrier gas type and flow, residence time, and reactor type [13]. Co-pyrolysis is simultaneously processing biomass with other materials such as coal, plastics, tires, sludge, etc. [14]. The main goal of co-pyrolysis is to get a synergistic effect between two feedstocks, but the extent of this synergy also depends upon the properties of feedstocks and operation parameters as in individual material pyrolysis [15]. Since biomass and coal have different properties, their co-pyrolysis also has different reactions and product distribution. In addition, the existence and extent of synergy between two feedstocks are controversial issues in the literature [16]. Therefore, co-pyrolysis of OP and coal needs to be investigated by using thermogravimetric analysis (TGA) and

Fourier transform infrared (FTIR) spectrometer integrated systems to thoroughly understand the mechanism and use this knowledge in industrial applications.

The analysis of the change in the mass of a substance depending on time or temperature is called TGA. The TGA is one of the most important techniques used to determine the thermal behavior of carbon-containing materials such as OP and coal. The thermal behavior of materials is estimated, for example, by measuring the weight loss as a function of time or temperature. Chemical composition, heating rate, atmosphere, temperature, and inorganic matter content are effective on the thermal behavior of biomass [17-18]. The composition of the evolved gases such as CO, CO₂, H₂, and CH₄ and functional groups can be identified by FTIR. Therefore, coupling TGA with FTIR is a useful tool in the simultaneous and continuous time-dependent analysis of mass loss (ML) change and evolution of gases produced during pyrolysis [19-21].

Several studies have been conducted by using OP as feedstock such as hydrothermal carbonization [9], biofuel production by combustion and/or gasification [22-24], thermal decomposition and/or kinetic analyses by combustion and/or gasification [25-30], biofuel production by pyrolysis [8, 10, 22, 31-37], pyrolytic thermal decomposition and kinetic analyses [17, 37-41]. Among the studies on the pyrolytic thermal decomposition, only [38] studied co-pyrolysis of OP with refuse-derived fuel - RDF (composed of 66% textile waste, 17.1% paper, 13.3% plastic bag, and 3.6% PET plastics) for three different blends (25, 50, and 75% of RDF). Besides, a study on synergistic effects during co-pyrolysis of OP and coal is missing among these studies. Furthermore, greenhouse gases (GHGs) released during the pyrolysis of OP, coal, and their blends have not been identified in these studies. This research hypothesizes that OP, coal, and their blends during pyrolysis have different thermal behaviors, synergistic effects, and evolved gas emissions investigated by the TGA/FTIR system. This study aims to provide a comprehensive analysis of thermal decomposition behavior, synergistic effects, and evolved gas analysis during pyrolysis of OP, coal, and their five different blends by using a TGA/FTIR integrated system, which is crucial for pilot/industrial-scale applications of energy production and climate change.

The objectives of this study were to: i) analyze the thermal decomposition behavior of pyrolysis of OP, coal, and their blends (0, 20, 40, 50, 60, 80, and 100% OP) at the heating rate (β) of (10, 20, 30, and 40°C min⁻¹) by using TGA, ii) investigate synergistic effects during co-pyrolysis of OP and coal, and iii) analyze evolved gases (CO, CO₂, CH₄, NO_x, and SO₂) released from TGA by directly giving to FTIR, which is integrated to the TGA. The results of this study can contribute to a better understanding of the pyrolysis characteristics of OP, coal, and their blends and provide useful knowledge for the design of industrial pyrolysis reactors.

MATERIALS AND METHODS

Materials

The OP used in this study was obtained from the ZemZem olive oil factory, which is around 30 km away from the Antalya city center in Türkiye. The ZemZem olive oil factory uses a two-stage extraction process that results in approximately 247.4 kg of oil, 735 kg of OP, and 200-300 L of wastewater per 1000 kg of olives. Based on the olive oil extraction technique there are three types of OP: i) the traditional technique which applies mechanical pressing and producing water, oil, and pomace; ii) the two-stage extraction process with no water application and generating oil and OP; and iii) the three-stage extraction process with crushing OP, adding water, and centrifugation, and therefore, producing water, oil, and OP [9]. The OP taken from the factory with a high moisture content was laid on a plate on the roof of the Akdeniz University Engineering Faculty Building (“36° 53’ 47.4396” and “30° 38’ 58.2612”) and occasionally mixed by hand until it dries completely in the open air. The dried OP was ground in the mill located at the Laboratory of Environmental Engineering Department of Akdeniz University (“36° 53’ 47.4396” and “30° 38’ 58.2612”). After milling, OP was sieved using sieves with different apertures to obtain the desired biomass particle sizes. The OP with a particle size of 212-180 μm was used for proximate and component analyses, while OP with a particle size $< 100 \mu\text{m}$ was used for elemental, TGA, and FTIR analyses. All OP samples were kept in airtight containers until different analyses and TGA/FTIR experiments were performed.

The Soma Lignite Coal (simply called coal) used in this study was supplied by the Mineral Research and Exploration Institute in Türkiye. The coal supplied as wet was dried naturally in the Laboratory of the Environmental Engineering Department of Akdeniz University, ground in the mill, and finally sieved to obtain the desired particle size. Particle size between 212 and 180 μm was used for proximate and component analyses, while particle size $< 100 \mu\text{m}$ was used for elemental and TGA/FTIR experiments. Coal samples were kept in airtight containers until analyses and experiments were carried out.

The blends of OP and coal were prepared by weighing the corresponding amounts of each feedstock directly in the TGA crucible and completely mixing using a fine needle to finally obtain the blend samples of 20% OP + 80% Coal, 40% OP + 60% Coal, 50% OP + 50% Coal, 60% OP + 40% Coal, and 80% OP + 20% Coal. The blending process was made just before the TGA/FTIR experiment to avoid changes in homogeneity and the properties of the blend with time. The percentage of OP added was selected in a broad range so that the effect of OP on the blend behavior was thoroughly investigated.

Feedstocks Characterization

Proximate analyses for the determination of moisture, ash, and volatile matter contents of OP and coal

were carried out at the Laboratory of Environmental Engineering Department of Akdeniz University according to ASTM standards of [42-44] respectively. The fixed carbon content of OP and coal was then calculated from the difference. Ultimate analysis of OP and coal was carried out at the Laboratory of Scientific and Technological Research Center of İnönü University (“38° 20’ 12” North and “38° 25’ 48” East) by using the CHNS-932 LECO Element Analyzer. After the C, H, N, and S percentages in OP and coal samples were determined simultaneously, the O percentage was calculated by using the difference. By using the ultimate analysis results the higher heating value (HHV) of the feedstocks was calculated by using the equation of [45]. Components such as cellulose, hemicellulose, lignin, and extractive contents were determined at the Laboratory of the Environmental Engineering Department of Akdeniz University after extraction of OP based on the ASTM standard [46]. The cellulose content was determined according to the method of [47], whereas the lignin content was determined based on the ASTM standard [48]. The hemicellulose content was calculated from the difference between cellulose plus lignin percentage and 100.

TGA/FTIR Experiments

The studies on the thermal behavior and evolution of gases during pyrolysis of OP, coal, and blends of these two in different ratios were carried out by the TGA/FTIR system (Fig. 1), which is the integrated version of Perkin Elmer Pyris STA 600 TGA and Spectrum 1 FTIR Spectrometer, in the Thermal Analysis Laboratory of the Middle East Technical University (“39° 53’ 31.4016” and “32° 46’ 42.9960”). In the TGA/FTIR experiments, samples ranging from 20 to 30 mg were heated from room temperature to 950°C (until the mass loss is stable) in the experiments with



TGA FTIR

Figure 1. Experimental device of TGA/FTIR integrated system.

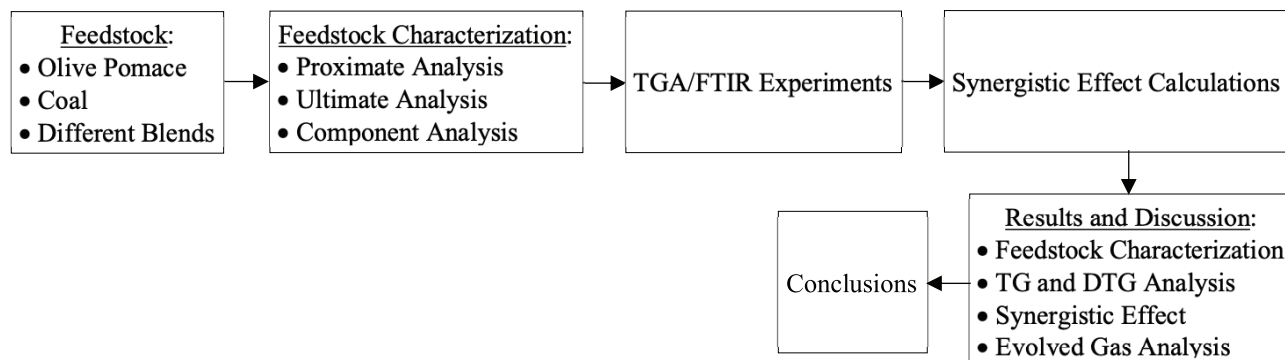


Figure 2. The flow chart showing the methodology used in this study.

a carrier (nitrogen) gas (99.99% purity) flow rate of 100 mL min⁻¹ and heating rates of 10, 20, 30, and 40°C min⁻¹. The temperature of the sample was measured by a thermocouple attached to the crucible. Before each experiment to eliminate systematic errors of the instrument a blank test was performed to obtain a baseline. All experiments were conducted at least twice to confirm the reproducibility of the results. The gases released during TGA of pyrolysis of OP, coal, or their blends were directed to the FTIR gas cell by using a transfer line. The balance adapter, the transfer line, and the FTIR gas cell were pre-heated up to 200°C to prevent condensation of volatiles and decompose all complexes. The gases released were determined by the FTIR spectra at a rate of 8 scans/sampling, a resolution of 4 cm⁻¹, and a wavelength range of 4000-400 cm⁻¹ from room temperature to 950°C.

Synergistic Effect

A synergistic effect between two feedstocks can be investigated by using the deviation. Deviation is defined as the difference between the experimental and calculated values of maximum ML rate (DTG_{max}), ML, and final residue (FR). It can be calculated by Eq. (1) [49-50].

$$\text{Deviation}(\%) = \frac{\text{Exp}_{\text{value}} - \text{Cal}_{\text{value}}}{\text{Exp}_{\text{value}}} \cdot 100 \quad (1)$$

where Exp_{value} is the experimental value obtained from the TG/DTG (thermogravimetry or ML/derivative thermogravimetry or ML) curve of the blend and Cal_{value} is the value calculated as the sum of the TG/DTG curves of each sample according to the ratio as expressed in Eq. (2).

$$\text{Cal}_{\text{value}} = (\text{Exp}_{\text{OP}} \cdot \lambda_{\text{OP}}) + (\text{Exp}_{\text{coal}} \cdot \lambda_{\text{coal}}) \quad (2)$$

where Exp_{OP} and Exp_{coal} are the experimental values of OP and coal obtained from the TG/DTG curve of each feedstock, whereas λ_{OP} and λ_{coal} are the proportion of OP and coal in the blend. The methodology used in this study was summarized in a flowchart (Fig. 2).

RESULTS AND DISCUSSION

Feedstock Characterization

Characterization results of OP and coal including proximate, ultimate, and component analyses are presented in Table 1. Moisture contents of OP and coal were significantly less than 10%, indicating that both feedstocks are suitable for thermochemical processing [51]. The moisture content of OP in this study was higher than the reported studies [29, 36-38] but lower than the studies [8, 9, 32, 39, 41]. The higher volatile matter content of OP (79.71%) compared to

Table 1. Main characteristics of feedstock

	Olive Pomace	Coal
Proximate Analysis		
Moisture (%)	4.23	5.31
Volatile matter (%)	79.71	26.93
Fixed carbon (%)	12.92	16.50
Ash (%)	3.13	51.26
Ultimate Analysis		
C (%)	59.43	30.33
H (%)	8.97	3.16
O (%)	29.83	65.23
N (%)	1.67	0.49
S (%)	0.10	0.79
H/C	0.15	0.10
O/C	0.50	2.15
HHV (MJ kg ⁻¹)	27.68	3.13
Component Analysis		
Cellulose (%)	27.94	
Hemicellulose (%)	29.84	
Lignin (%)	33.87	
Extractives (%)	37.61	

C: Carbon, H: Hydrogen, O: Oxygen (calculated by difference as 100 - (total of C, H, N, and S%), N: Nitrogen, S: Sulphur, and HHV: Higher heating value.

coal (26.93%) was an indication of a higher yield of either condensable or non-condensable biofuels of OP [52]. The volatile matter content of this study was the highest among the studies [8, 9, 17, 26, 32, 36-39, 41].

High C and H contents and HHV value but low O content of OP showed its high energy potential. However, the opposite was true for coal, where low C and H contents but high O content, which resulted in lower HHV value, reduced the energy potential of coal (Table 1). The higher HHV value of OP in this study than that of the studies [9, 26, 32, 37, 38] also proved its high energy potential. On the other hand, the higher N content of OP and higher S content of coal showed their potential for emission to the environment. When the proximate and ultimate analysis results were evaluated in general, it showed us that co-pyrolysis

could be an opportunity to eliminate the negative properties of both OP and coal. Component analysis results (Table 1) of OP showed that cellulose, hemicellulose, and lignin contents were almost equally distributed. The lignin content of OP in this study was similar to the reported studies [9, 26, 32, 36, 39]. The relatively high lignin content showed that the pyrolysis or co-pyrolysis method was the right choice for this study because pyrolysis has a high capacity for the conversion of resistant materials like lignocellulosic biomass.

TG and DTG Analysis

The TG and DTG curves and corresponding characteristic temperatures associated with MLs in different stages of decomposition during pyrolysis of OP, coal, and their blends at different heating rates are presented in Figure 3

Table 2. Characteristic temperatures associated with mass losses in different stages of decomposition during pyrolysis of olive pomace, coal, and their blends at different heating rates

Blend Ratio	β	T_{\min}	ML-I	T_1	ML-II	T_2	ML-III	T_3	T_{\max}	FR
	$^{\circ}\text{C min}^{-1}$	$^{\circ}\text{C}$	(%)	$^{\circ}\text{C}$	(%)	$^{\circ}\text{C}$	(%)	$^{\circ}\text{C}$	$^{\circ}\text{C}$	(%)
0% OP + 100% Coal	10	30	6.33	250	15.87	630	6.59	770	939	68.86
	20		5.87	260	15.60	650	6.49	810	936	70.89
	30		4.80	270	16.08	670	6.65	850	937	71.78
	40		4.08	290	16.69	700	6.42	900	934	72.57
20% OP + 80% Coal	10	30	5.83	170	27.45	630	5.90	795	941	59.02
	20		6.50	210	25.24	685	6.10	855	937	60.88
	30		6.90	250	26.30	700	5.44	900	935	61.05
	40		8.23	285	25.48	730	4.82	930	934	61.44
40% OP + 60% Coal	10	30	5.14	170	38.31	630	5.07	780	940	52.81
	20		6.34	195	38.47	670	4.63	840	938	49.79
	30		4.52	215	38.48	685	4.70	870	935	51.85
	40		7.59	245	36.75	720	5.06	920	935	50.44
50% OP + 50% Coal	10	30	3.88	160	45.89	620	4.32	760	940	43.73
	20		3.19	175	44.94	650	4.11	780	938	46.33
	30		3.57	185	44.93	665	4.17	810	934	46.37
	40		3.35	195	45.07	690	4.18	850	932	46.84
60% OP + 40% Coal	10	30	3.58	150	56.07	610	3.55	750	941	34.73
	20		2.90	160	52.92	645	3.52	780	936	39.39
	30		5.14	180	50.97	660	3.58	805	935	39.41
	40		4.29	190	54.45	680	3.17	820	932	37.38
80% OP + 20% Coal	10	30	4.24	140	65.17	610	2.64	740	941	35.67
	20		5.03	160	65.26	640	2.33	775	936	30.41
	30		5.56	165	62.85	650	2.46	795	931	28.28
	40		8.01	230	61.46	680	2.94	900	931	27.36
100% OP + 0% Coal	10	30	4.96	140	76.34	550	1.91	740	932	15.35
	20		5.83	175	76.00	590	1.61	765	929	15.54
	30		6.32	200	75.61	620	1.37	790	928	16.03
	40		7.04	220	75.10	670	1.21	850	926	16.36

OP: Olive Pomace; β : heating rate; ML: mass losses at the decomposition stages I, II, and III; FR: final residues.

and Table 2, respectively. Even though the decomposition was affected by different parameters such as temperature, heating rate, and blend ratio in varying degrees; in general, three main stages were observed during the decomposition of OP, coal, and their blends through pyrolysis (Fig. 3). The first stage was attributed to the removal of water and some extractives from the sample and was almost constant with

the corresponding temperature $< 180^{\circ}\text{C}$ as reported by [37]. At the same heating rate of $40^{\circ}\text{C min}^{-1}$ for the first stage, the highest ML was observed as 8.23% in the blend of 20% OP + 80% Coal, while the lowest ML was recorded as 3.35% in the blend of 50% OP + 50% Coal (Table 2), which was similar to water evaporation. The second stage was related to the removal of volatile components from the sample

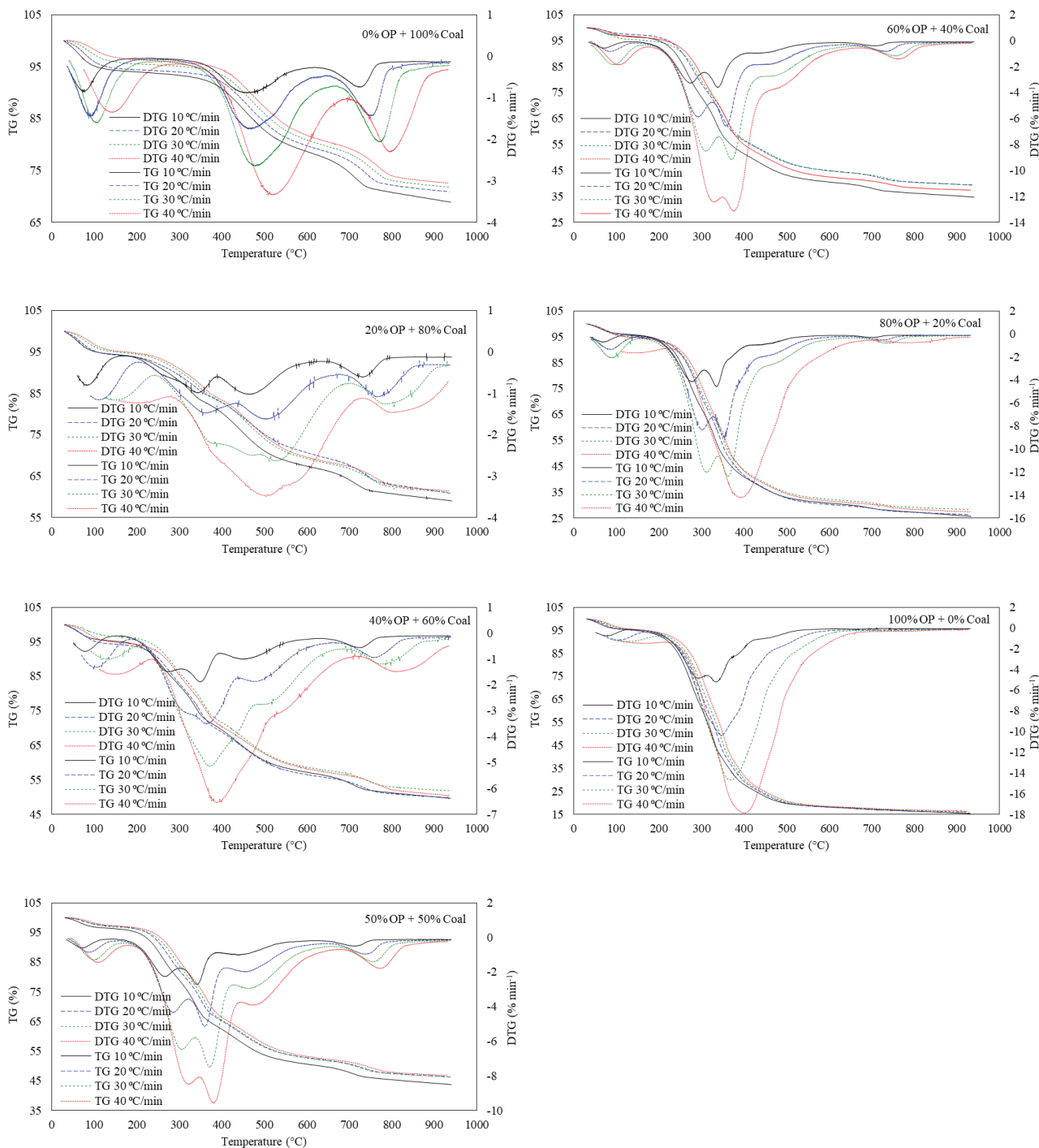


Figure 3. TG and DTG curves of pyrolysis of olive pomace, coal, and their blends at different heating rates.

and the main pyrolysis process took place in this stage. The third stage was associated with the removal of components such as lignin that were not easily broken down. At the end of the third stage, biochar formation was observed. The second and third stages took place in different temperature ranges as OP content increased in the blends (Table 2).

Pyrolysis of pure coal had three decomposition stages with an average ML of 16.06% and a temperature range of 270-660°C in the second stage and an average ML of 6.54% and a temperature range of 660-830°C in the third stage. On the other hand, pyrolysis of pure OP had no third stage, but it had a significant second stage, associated with the devolatilization of the main components, with the highest

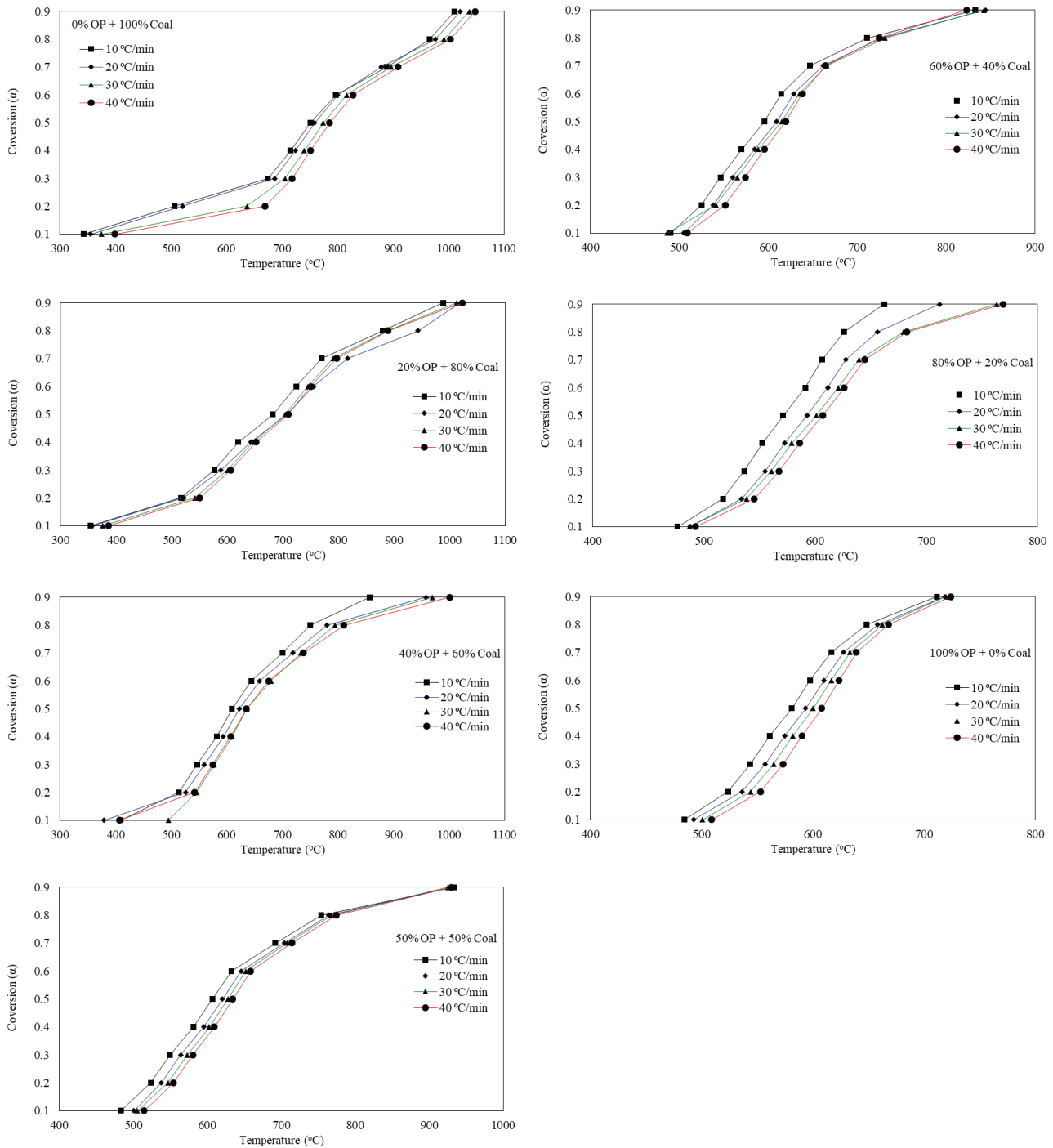


Figure 4. Relationship between mass conversion degree and temperature for pyrolysis of olive pomace, coal, and their blends at different heating rates.

average ML of 75.76% and a narrower temperature range of 180–600°C [37]. Most of the volatiles were released between 200 and 400°C. The lignin started decomposition at 400°C and continued up to the ultimate pyrolysis temperature of 600°C (Aissaoui et al., 2023, [37]). The devolatilization almost finished after 600°C and there was no additional ML [34, 37].

As can be seen in Figure 3 and Table 2, ML systematically increased in the second stages of all blends from pure coal towards pure OP [53], but the corresponding temperatures and temperature ranges decreased, indicating a high reactivity [29]. The thermal decomposition took place at lower temperatures compared to coal as OP content increased in the blend possibly due to the catalytic effect of minerals such as potassium and sodium on the thermal decomposition of the blends. However, the opposite was true for the third stage, where MLs systematically decreased. In the third stage, biochar or FR formation decreased in the blends from pure coal to pure OP. The lowest FR was observed in pure pomace at a maximum temperature of 932 and 926°C with amounts varying between 15.35% and 16.36%, respectively. The FR formed in pure coal reached up to 72.57% at a maximum temperature of 934°C. The DTG curves of the samples with different peaks in specific

temperature ranges indicate that the pyrolysis process cannot be described by a single thermal decomposition stage, but the process of each sample shows multi-stage reactions. These results indicate that OP, coal, and their blends have different thermal decomposition characteristics during pyrolysis due to the complex nature of the samples resulting from overlapping zones of cellulose, hemicellulose, and lignin decomposition as reported by [54]. Furthermore, it can be concluded that as the OP content in the blend increases biofuel potential increases due to higher ML or volatiles, but biochar potential decreases due to lower FR.

The DTG curves of all blends showed two distinct peaks in the second stage (Fig. 3). The highest peak of DTG was observed between 300 and 400°C. The first peak is mainly due to the pyrolysis of the less stable hemicellulose, while the second peak is attributed to the pyrolysis of cellulose. The almost equal amounts of cellulose and hemicellulose in OP can be related to the similarity between the peaks. On the other hand, lignin decomposition is represented by the long tail [40]. In general, the shape of the DTG curve is largely dependent on the percentage of cellulose, hemicellulose, lignin, and minerals during pyrolytic thermal degradation [55]. A peak shift towards higher decomposition temperatures was observed with an increased heating

Table 3. Synergistic effect calculation for mass loss, maximum mass loss rate, and final residue during co-pyrolysis of olive pomace and coal

Blend Ratio	β °C min ⁻¹	Experimental			Calculated			Deviation		
		DTG _{max}	ML (%)	FR (%)	DTG _{max}	ML (%)	FR (%)	DTG _{max}	ML (%)	FR (%)
20% OP + 80% Coal	10	1.01	33.35	59.02	1.73	33.62	58.16	-0.418	-0.008	0.015
	20	1.60	31.34	60.88	3.45	33.19	59.82	-0.536	-0.056	0.018
	30	2.61	31.74	61.05	5.02	33.58	60.63	-0.480	-0.055	0.007
	40	3.46	30.30	61.44	6.22	33.75	61.33	-0.444	-0.102	0.002
40% OP + 60% Coal	10	1.82	43.38	52.81	2.59	44.78	47.46	-0.297	-0.031	0.113
	20	3.48	43.10	49.79	5.16	44.30	48.75	-0.326	-0.027	0.021
	30	5.11	43.18	51.85	7.42	44.43	49.48	-0.311	-0.028	0.048
	40	6.52	41.81	50.44	9.12	44.39	50.09	-0.285	-0.058	0.007
50% OP + 50% Coal	10	2.68	50.21	43.73	3.02	50.36	42.11	-0.111	-0.003	0.039
	20	5.11	49.05	46.33	6.02	49.85	43.22	-0.151	-0.016	0.072
	30	7.38	49.10	46.37	8.62	49.86	43.91	-0.143	-0.015	0.056
	40	9.49	49.25	46.84	10.57	49.71	44.47	-0.102	-0.009	0.053
60% OP + 40% Coal	10	3.55	59.62	34.73	3.44	55.93	36.75	0.031	0.066	-0.055
	20	6.47	56.44	39.39	6.88	55.40	37.68	-0.059	0.019	0.045
	30	9.04	54.55	39.41	9.81	55.28	38.33	-0.079	-0.013	0.028
	40	13.01	57.62	37.38	12.01	55.03	38.84	0.083	0.047	-0.038
80% OP + 20% Coal	10	4.47	67.81	35.67	4.30	67.09	26.05	0.041	0.011	0.369
	20	8.94	67.59	30.41	8.59	66.51	26.61	0.040	0.016	0.143
	30	12.23	65.31	28.28	12.21	66.13	27.18	0.001	-0.012	0.040
	40	14.18	64.40	27.36	14.91	65.67	27.60	-0.049	-0.019	-0.009

OP: Olive Pomace, β : Heating rate, DTG_{max}: Maximum mass loss rate, ML: Mass loss, FR: Final residual.

rate. However, in general, the shapes of DTG curves were not changed with the heating rate from 10 to 40°C min⁻¹. The heat and mass transfer limitations that cause temperature gradients within the particle result in the shift of the decomposition curves. Increasing the heating rate does not allow good temperature stabilization in the sample [40]. The same behavior has been reported for other biomass feedstocks in the literature such as palm residues [56], Arundo Donax [57], and sawdust [55].

The α -temperature relationship for pyrolysis of OP, coal, and their blends at different β values showed a clear relation between α and temperature (Fig. 4). For a specific β , as temperature increased α also increased, indicating a more conversion of the sample. Similarly, for a specific α , as temperature increased β also increased. Even though there were variations among the blends, the main conversion was observed between 500 and 700°C.

Synergistic Effect

Synergistic effects were calculated for different blends and β values, ML, DTG_{max}, and FR during co-pyrolysis of olive pomace and coal; and the results are presented in Table 3. A positive deviation value indicates a synergistic effect, whereas a negative deviation value states no synergy between two feedstocks [58]. A synergistic effect was observed between OP and coal for FR (biochar formation) in all β values of all blends except at three β values of the last two blends (60% OP + 40% Coal and 80% OP + 20% Coal). For ML and DTG_{max}, there was no synergy between OP and coal for the first three blends (20% OP + 80% Coal, 40% OP + 60% Coal, and 50% OP + 50% Coal). However, a synergistic effect was observed for ML and DTG_{max} in all β values of the last two blends (60% OP + 40% Coal and 80% OP + 20% Coal) except at three β values of each. These results indicate that the blends of 60% OP + 40% Coal and 80% OP + 20% Coal can be used to create a synergistic effect between OP and coal for ML and DTG_{max} during pyrolysis. This synergy was also supported by the fact that MLs systematically increased and the corresponding temperatures and temperature ranges decreased as OP content increased in the blends (Fig. 3).

The synergistic effect increased with the increase of the percentage of OP in the blend during pyrolysis due to the release of hydrogen and hydroxy radicals and the catalytic effects of alkali and alkaline earth metals in materials [59]. The released hydrogen and hydroxyl radicals from biomass can function as a catalyst for these reactions. The reaction rate increases and the activation energy decreases with the beginning of hydrogen formation [60]. High components obtained from the volatilization of biomass in the blends with high amounts of biomass also support the volatilization of coal. Therefore, the yield of bio-oil and gas increases but the solid product yield decreases as the amount of biomass in the blend increases [61]. These results indicate that some interaction may occur between OP and coal, therefore, the

thermal behavior of the blend cannot be defined by just adding the thermal behavior of OP and coal [62].

Evolved Gas Analysis by TGA/FTIR

The 3D FTIR spectrum of TGA/FTIR experiments for pyrolysis products of OP and coal at the β of 30°C min⁻¹ is presented in Figure 5 to display the spectral intensity or absorbance, corresponding to the vibration of different chemical bonds and functional groups corresponding to the evolved gases, with temperature and wavenumber or wavelength. A relatively high β of 30°C min⁻¹ was selected to obtain quality FTIR data [63]. The studied gases released during the pyrolysis of OP, coal, and their blends were CO, CO₂, CH₄, NO_x, and SO₂ and the corresponding wavelength values were 2178, 2400-2240, 3016, 1762, and 1342 cm⁻¹, respectively [64]. The TGA/FTIR spectrum of the samples showed different peaks related to different functional groups. The intense peak of the coal sample is related to the characteristic peak of C=O vibration which represents CO₂ due to the decarboxylation reactions of carboxylic acid groups. The C-H stretching vibrations are due to the presence of light hydrocarbon gases like CH₄. Beer-Lambert's law states that there is a linear relationship between spectral absorbance at a given wavenumber and the concentration of gaseous species. Based on this law, the gases that evolved during the pyrolysis of OP had an overall (about 10 times) higher concentration than that of coal (Fig. 5).

The FTIR spectrum of different gases as a function of temperature from pyrolysis of OP, coal, and their blends are illustrated in Figure 6. Besides, the peak absorbance values and corresponding temperatures for different evolved gases and blend ratios were tabulated in Table 4. The profiles of evolved gases seen in Figure 6 were very similar to the DTG curves (Fig. 3) obtained at the same β during TGA [65]. In the absorbance of CO, the first group of peaks was observed at temperatures of 200-400°C with a maximum at 280°C which corresponds to the decomposition of hemicellulose and cellulose, whereas the second group of peaks was shown at temperatures of 400-600°C with a maximum at 580°C that represents the lignin decomposition as discussed in the TG and DTG results. The highest peak intensity with the largest contribution to CO emission was observed in the pure OP sample, whereas the lowest peak with the least contribution was observed in the 40% OP + 60% Coal sample. Similar behavior was observed in the CO₂ absorbance, but the trends were not as clear as the CO absorbance (Fig. 6, Table 4). The TG and DTG curves and the emission profiles of CO and CO₂ had similar patterns, indicating that these two gases are released during the entire pyrolysis decomposition temperature range. In particular, between 200 and 400°C, the CO and CO₂ peaks coincided with the two peaks observed in the DTG curves.

The absorbances of CH₄, NO_x, and SO₂ were different from those of CO and CO₂ in terms of the number and intensity of peaks. The absorbances of these gases showed similar and smooth trends with a single peak at

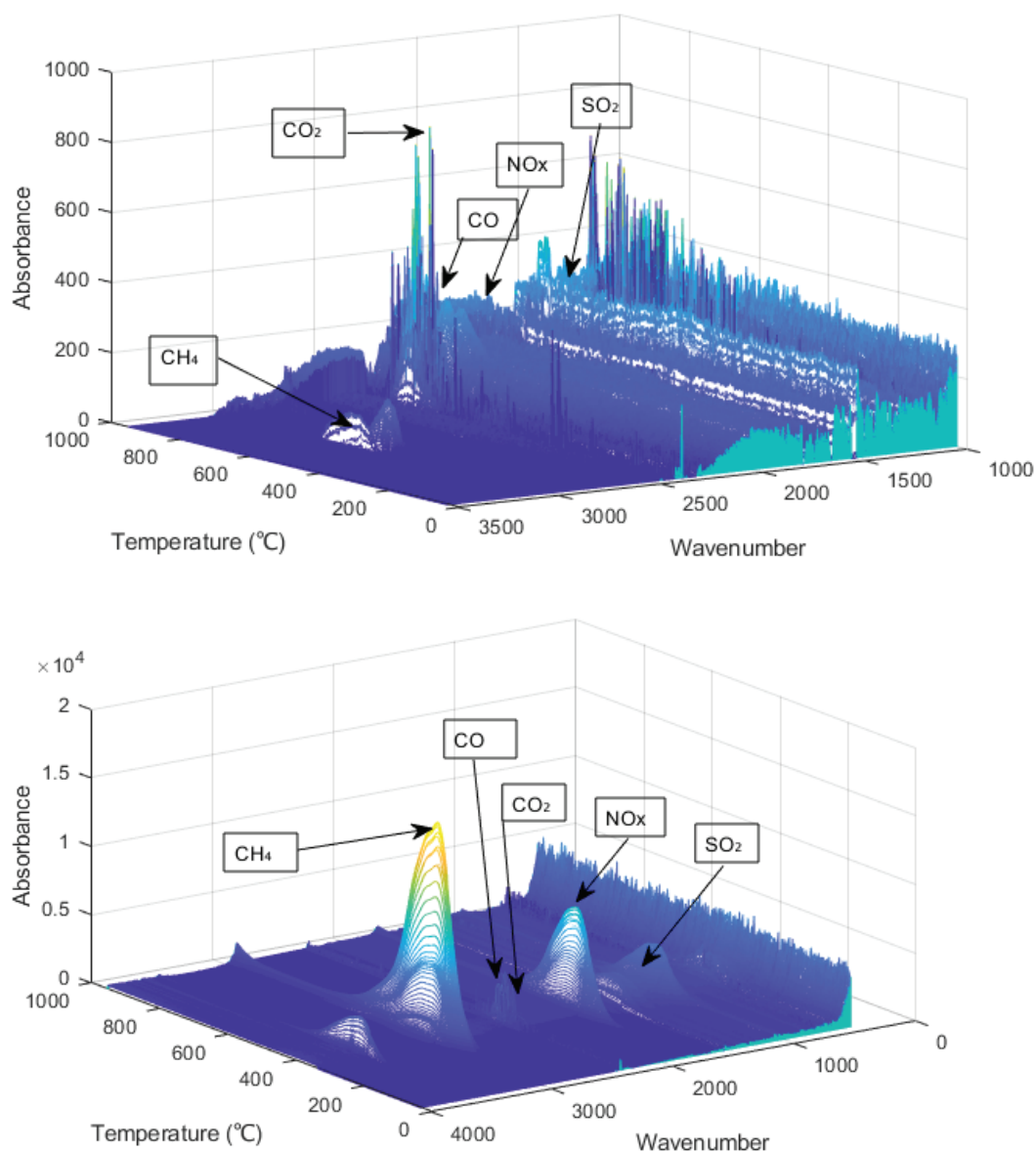


Figure 5. 3D infrared spectrum of pyrolysis products for coal (top) and olive pomace (bottom) at a heating rate of 30 °C min⁻¹.

temperatures of 200-600°C, representing hemicellulose, cellulose, and lignin decompositions at corresponding temperatures as mentioned in TG and DTG curves. The initial emission between 200 and 300°C was associated with hemicellulose degradation and NO_x and SO₂ peaks were observed in this temperature range. The second emission observed between 300 and 400°C was related to the thermal degradation of cellulose [66-67]. The CH₄ emission at slightly higher temperatures may be due to lignin degradation, as well as coal decomposition, which continues to emit light volatiles at higher temperatures. It is seen that the peak intensity and hence the contribution to CH₄, NO_x, and SO₂ emissions increased as the OP content increased

in the blend. Ghouma et al. [40] showed that the gases released during the OP pyrolysis represented about 20% of the initial mass of OP. About 50% of the original OP was converted into other products such as tar, persistent gases, and water. Besides, the amounts obtained were slightly higher than those found in this study. However, there was a fundamental difference between the study conducted by Ghouma et al. [40] and this study. While olive oil is produced with a three-stage extraction process in Tunisia, it is produced with a two-stage extraction process in Türkiye. Also, Ghouma et al. [40] treated OP residue with hexane to extract oil. This refers to the emission of lower carbonic compounds during pyrolysis.

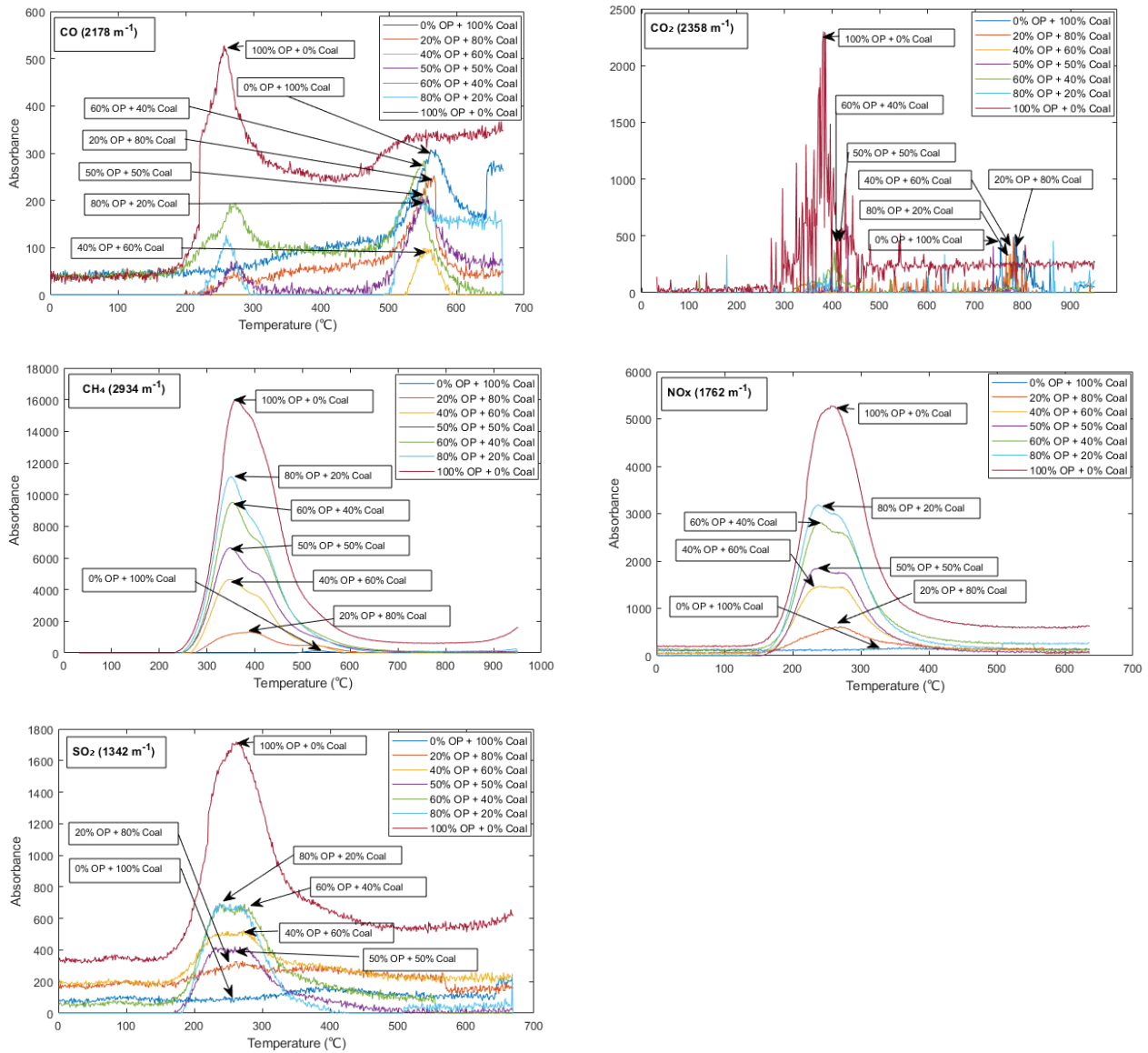


Figure 6. FTIR spectrum of different gases as a function of temperature from pyrolysis of olive pomace, coal, and their blends.

Table 4. The peak absorbance values and corresponding temperatures for different evolved gases and blend ratios

Blend Ratio	CO		CO ₂		CH ₄		NO _x		SO ₂	
	T	A	T	A	T	A	T	A	T	A
0% OP + 100% Coal	570	300	750	500	530	150	350	200	250	90
20% OP + 80% Coal	575	250	790	500	390	1200	270	600	250	320
40% OP + 60% Coal	560	100	780	500	350	4500	230	1500	280	500
50% OP + 50% Coal	560	210	410	500	350	6500	230	1800	260	400
60% OP + 40% Coal	540	290	400	500	350	9500	230	2800	270	650
80% OP + 20% Coal	550	200	770	330	350	11250	230	3200	240	670
100% OP + 0% Coal	250	520	390	2300	350	16000	250	5200	250	1700

OP: Olive Pomace, T: Temperature (°C), Absorbance (m⁻¹).

CONCLUSION

In this study, the thermal behavior and evolved gas of OP, coal, and their five blends at four β values during pyrolysis were analyzed by using TGA/FTIR. In addition, the synergistic effects during the co-pyrolysis of OP and coal were investigated. The feedstock characterization results showed the high energy potential of OP with high C (59.43%) and volatile matter (79.71%) contents and HHV of 27.68 MJ kg⁻¹. When coal is considered a feedstock with its relatively low C (30.33%) content and HHV (3.13 MJ kg⁻¹), co-pyrolysis of OP and coal could be an opportunity to eliminate the negative properties of coal for energy production and the environment.

In the second decomposition stage of all samples from pure coal toward pure OP, systematically increasing ML and decreasing respective temperatures and temperature ranges indicate an increasing reactivity. However, both ML and FR systematically decreased in the third decomposition stage of all samples as OP content increased in the blend. It can be concluded that as the OP content in the blend increases biofuel potential increases due to higher ML or volatiles, but biochar potential decreases due to lower FR. The synergistic effects observed between OP and coal for the blends of 60% OP + 40% Coal and 80% OP + 20% Coal indicate that these blends can be used to get rid of the adverse effects of low-value coal during co-pyrolysis as well as evaluating it in energy production.

The CO and CO₂ had similar absorbance profiles, whereas the absorbances of CH₄, NO_x, and SO₂ showed similar and clear trends with a single peak at temperatures of 200–600°C, representing hemicellulose, cellulose, and lignin decompositions at corresponding temperatures as in TG and DTG curves. The FTIR spectrum of the blends showed different peaks, whereas the OP content increased in the blend the peak intensity and therefore the contribution to CH₄, NO_x, and SO₂ emission increased. Overall, since each sample (pure OP and coal, and their blends) had different thermal behavior, synergistic effects, and evolved gases; further study on the co-pyrolysis of OP and coal with more specific blends and different experimental parameters may be useful for effective pyrolysis process and better waste management.

NOMENCLATURE

Abbreviations

3D	Three dimensional
ASTM	American Society for Testing and Materials
C	Carbon
CH ₄	Methane
CO	Carbon monoxide
CO ₂	Carbon dioxide
DTG	Differential thermogravimetry
Eq.	Equation
FR	Final residue
FTIR	Fourier Transform Infra Red

GHG	Greenhouse gas
H	Hydrogen
H ₂	Hydrogen gas
HHV	Higher heating value
METU	Middle East Technical University
ML	Mass loss
N	Nitrogen
NO _x	Nitrogen oxide
O	Oxygen
OP	Olive pomace
RDF	Refuse driven fuel
S	Sulphur
SO ₂	Sulphur dioxide
TG	Thermogravimetry
TGA	Thermogravimetric analysis

Symbols and Units

α	Mass conversion degree
β	Heating rate
Cal _{value}	Calculated value
DTG _{max}	Maximum differential thermogravimetry
Exp _{coal}	Experimental values of coal
Exp _{OP}	Experimental values of OP
Exp _{value}	Experimental value
λ_{OP}	Proportion of OP
λ_{coal}	Proportion of coal

ACKNOWLEDGEMENTS

This work was financially supported by the Scientific Research Projects (BAP) Division of Akdeniz University in Türkiye with the project number of FYL-2022-5735.

AUTHORSHIP CONTRIBUTIONS

Hasan Merdun: Conceptualization, Funding acquisition, Investigation, Project administration, Resources, Software, Supervision, Validation, Writing - review & editing.

Balkıs Yahyaoui: Data curation, Formal analysis, Investigation, Methodology, Visualization.

DATA AVAILABILITY STATEMENT

The authors confirm that the data that supports the findings of this study are available within the article. Raw data that support the finding of this study are available from the corresponding author, upon reasonable request.

CONFLICT OF INTEREST

The authors declared no potential conflicts of interest with respect to the research, authorship, and/or publication of this article.

ETHICS

There are no ethical issues with the publication of this manuscript.

REFERENCES

- [1] Cabeza LE, Palacios A, Serrano S, Ürge-Vorsatz D, Barreneche C. Comparison of past projections of global and regional primary and final energy consumption with historical data. *Renewable Sustainable Energy Rev* 2018;82:681-688. [\[CrossRef\]](#)
- [2] Parascanu MM, Puig Gamero M, Sánchez P, Soreanu G, Valverde JL, Sanchez-Silva L. Life cycle assessment of olive pomace valorisation through pyrolysis. *Renewable Energy* 2018;122:589-601. [\[CrossRef\]](#)
- [3] Valenti F, Porto SMC, Selvaggi R, Pecorino B. Co-digestion of by-products and agricultural residues: A bioeconomy perspective for a Mediterranean feedstock mixture. *Sci Total Environ* 2020;700:134440. [\[CrossRef\]](#)
- [4] Yanik DK. Alternative to traditional olive pomace oil extraction systems: Microwave-assisted solvent extraction of oil from wet olive pomace. *LWT-Food Sci Technol* 2017;77:45-51. [\[CrossRef\]](#)
- [5] IOC. International Olive Council. Available at: <https://www.internationaloliveoil.org/>. Accessed May 01, 2021.
- [6] Mosaiquefm. Available at: <https://www.mosaiquefm.net/>. Accessed Dec 12, 2021.
- [7] Biomass Energy Potential Atlas (BEPA). The Directorate General of Renewable Energy, the Republic of Türkiye Ministry of Energy and Natural Resources, Ankara, Türkiye; 2019.
- [8] Volpe M, D'Anna C, Messineo S, Volpe R, Messineo A. Sustainable production of bio-combustibles from pyrolysis of agro-industrial wastes. *Sustainability* 2014;6:7866-7882. [\[CrossRef\]](#)
- [9] Missaoui A, Bostyn S, Belandria V, Cagnon B, Sarh B, Gökalp I. Hydrothermal carbonization of dried olive pomace: Energy potential and process performances. *J Anal Appl Pyrolysis* 2017;128:281-290. [\[CrossRef\]](#)
- [10] Nunes LJR, Loureiro LMEF, Sá LCR, Silva HFC. Evaluation of the potential for energy recovery from olive oil industry waste: Thermochemical conversion technologies as fuel improvement methods. *Fuel* 2020;279:118536. [\[CrossRef\]](#)
- [11] McKendry P. Energy production from biomass (part 2): Conversion technologies. *Bioresour Technol* 2002;83:47-54. [\[CrossRef\]](#)
- [12] Das P, Chandramohan VP, Mathimani T, Pugazhendhi A. Recent advances in thermochemical methods for the conversion of algal biomass to energy. *Sci Total Environ* 2021;766:144608. [\[CrossRef\]](#)
- [13] Wang SR, Dai GX, Yang HP, Luo ZY. Lignocellulosic biomass pyrolysis mechanism: A state-of-the-art review. *Prog Energy Combust Sci* 2017;62:33-86. [\[CrossRef\]](#)
- [14] Ismail TM, Banks S, Yang Y, Yang H, Chen Y, Bridgwater A, et al. Coal and biomass co-pyrolysis in a fluidized-bed reactor: Numerical assessment of fuel type and blending conditions. *Fuel* 2020;275:118004. [\[CrossRef\]](#)
- [15] Hassan H, Lim J, Hameed B. Recent progress on biomass co-pyrolysis conversion into high-quality bio-oil. *Bioresour Technol* 2016;221:645-655. [\[CrossRef\]](#)
- [16] Wang G, Dai Y, Yang H, Xiong Q, Wang K, Zhou J, et al. A review of recent advances in biomass pyrolysis. *Energy Fuels* 2020;34:15557-15578. [\[CrossRef\]](#)
- [17] Özveren U, Özdoğan ZS. Investigation of the slow pyrolysis kinetics of olive oil pomace using thermo-gravimetric analysis coupled with mass spectrometry. *Biomass Bioenergy* 2013;58:168-179. [\[CrossRef\]](#)
- [18] Bach QV, Chen WH. Pyrolysis characteristics and kinetics of microalgae via thermogravimetric analysis (TGA): A state-of-the-art review. *Bioresour Technol* 2017;246:88-100. [\[CrossRef\]](#)
- [19] Shen DK, Gu S, Bridgwater AV. Study on the pyrolytic behaviour of xylan-based hemicellulose using TG-FTIR and Py-GC-FTIR. *J Anal Appl Pyrolysis* 2010;87:199-206. [\[CrossRef\]](#)
- [20] Dai Q, Jiang X, Lv G, Ma X, Jin Y, Wang F, et al. Investigation into particle size influence on PAH formation during dry sewage sludge pyrolysis: TG-FTIR analysis and batch scale research. *J Anal Appl Pyrolysis* 2015;112:388-393. [\[CrossRef\]](#)
- [21] Cai H, Liu J, Xie W, Kuo J, Buyukada M, Evrendilek F. Pyrolytic kinetics, reaction mechanisms and products of waste tea via TG-FTIR and Py-GC/MS. *Energy Convers Manag* 2019;184:436-447. [\[CrossRef\]](#)
- [22] Ferreira CIA, Calisto V, Cuerda-Correa EM, Otero M, Nadais H, Esteves VI. Comparative valorisation of agricultural and industrial biowastes by combustion and pyrolysis. *Bioresour Technol* 2016;218:918-925. [\[CrossRef\]](#)
- [23] Tamošiūnas A, Chouchène A, Valatkevicius P, Gimžauskaite D, Aikas M, Uscila R, et al. The potential of thermal plasma gasification of olive pomace charcoal. *Energies* 2017;10:710. [\[CrossRef\]](#)
- [24] Parascanu MM, Sanchez P, Soreanu G, Valverde JL, Sanchez-Silva L. Environmental assessment of olive pomace valorization through two different thermochemical processes for energy production. *J Clean Prod* 2018;186:771-781. [\[CrossRef\]](#)
- [25] Garcia-Ibanez P, Sanchez M, Cabanillas A. Thermogravimetric analysis of olive-oil residue in air atmosphere. *Fuel Process Technol* 2006;87:103-107. [\[CrossRef\]](#)
- [26] Buratti C, Mousavi S, Barbanera M, Lascaro E, Cotana F, Bufacchi M. Thermal behaviour and kinetic study of the olive oil production chain residues and their mixtures during co-combustion. *Bioresour Technol* 2016;214:266-275. [\[CrossRef\]](#)
- [27] Guizani C, Haddad K, Jeguirim M, Colin B, Limousy L. Combustion characteristics and kinetics of torrefied olive pomace. *Energy* 2016;107:453-463. [\[CrossRef\]](#)

- [28] Prestipino M, Galvagno A, Karlström O, Brink A. Energy conversion of agricultural biomass char: Steam gasification kinetics. *Energy* 2018;161:1055-1063. [\[CrossRef\]](#)
- [29] Puig-Gamero M, Lara-Díaz J, Valverde JL, Sánchez P, Sanchez-Silva L. Synergistic effect in the steam co-gasification of olive pomace, coal and petcoke: Thermogravimetric-mass spectrometric analysis. *Energy Convers Manag* 2018;159:140-150. [\[CrossRef\]](#)
- [30] Puig-Gamero M, Lara-Díaz J, Valverde JL, Sanchez-Silva L, Sánchez P. Dolomite effect on steam co-gasification of olive pomace, coal and petcoke: TGA-MS analysis, reactivity and synergistic effect. *Fuel* 2018;234:142-150. [\[CrossRef\]](#)
- [31] Encinar JM, Gonzalez JF, Martinez G, Roman S. Catalytic pyrolysis of exhausted olive oil waste. *J Anal Appl Pyrolysis* 2009;85:197-203. [\[CrossRef\]](#)
- [32] Duman G, Yanik J. Two-step steam pyrolysis of biomass for hydrogen production. *Int J Hydrogen Energy* 2017;42:17000-17008. [\[CrossRef\]](#)
- [33] Christoforou EA, Fokaides PA, Banks SW, Nowakowski D, Bridgwater AV, Stefanidis S, et al. Comparative study on catalytic and non-catalytic pyrolysis of olive mill solid wastes. *Waste Biomass Valorization* 2018;9:301-313. [\[CrossRef\]](#)
- [34] Dorado F, Sanchez P, Alcazar-Ruiz A, Sanchez-Silva L. Fast pyrolysis as an alternative to the valorization of olive mill wastes. *J Sci Food Agric* 2021;101:2650-2658. [\[CrossRef\]](#)
- [35] Kostas ET, Durán-Jiménez G, Shepherd BJ, Meredith W, Stevens LA, Williams OSA, et al. Microwave pyrolysis of olive pomace for bio-oil and bio-char production. *Chem Eng J* 2020;387:123404. [\[CrossRef\]](#)
- [36] Alcazar-Ruiz A, Garcia-Carpintero R, Dorado F, Sanchez-Silva L. Valorization of olive oil industry subproducts: Ash and olive pomace fast pyrolysis. *Food Bioprod Process* 2021;125:37-45. [\[CrossRef\]](#)
- [37] Aissaoui MH, Trabelsi ABH, Bensidhom G, Ceylan S, Leahy JJ, Kwapinski W. Insights into olive pomace pyrolysis conversion to biofuels and biochars: Characterization and techno-economic evaluation. *Sustainable Chem Pharm* 2023;32:10102. [\[CrossRef\]](#)
- [38] Kabakcı SB, Aydemir H. Pyrolysis of olive pomace and copyrolysis of olive pomace with refuse-derived fuel. *Environ Prog Sustain Energy* 2014;33:649-656. [\[CrossRef\]](#)
- [39] Guida MY, Bouaik H, Tabal A, Hannioui A, Solhy A, Barakat A, et al. Thermochemical treatment of olive mill solid waste and olive mill wastewater. *J Therm Anal Calorim* 2015;123:1657-1666. [\[CrossRef\]](#)
- [40] Ghouma I, Jeguirim M, Guizani C, Ouederni A, Limousy L. Pyrolysis of olive pomace: Degradation kinetics, gaseous analysis and char characterization. *Waste Biomass Valorization* 2017;8:1689-1697. [\[CrossRef\]](#)
- [41] Martín-Lara MA, Iáñez-Rodríguez I, Blázquez G, Quesada L, Pérez A, Calero M. Kinetics of thermal decomposition of some biomasses in an inert environment. An investigation of the effect of lead loaded by biosorption. *Waste Manag* 2017;70:101-113. [\[CrossRef\]](#)
- [42] ASTM D3173-03. Standard Test Method for Moisture in the Analysis Sample of Coal and Coke, ASTM International, West Conshohocken, PA; 2003.
- [43] ASTM D3174-02. Standard Test Method for Ash in the Analysis Sample of Coal and Coke from Coal. American Society for Testing and Materials; 2002.
- [44] ASTM D3175-07. Standard Test Method for Volatile Matter in the Analysis Sample of Coal and Coke. American Society for Testing and Materials; 2007
- [45] Channiwala SA, Parikh PP. A unified correlation for estimating HHV of solid, liquid and gaseous fuels. *Fuel* 2002;81:1051-1063. [\[CrossRef\]](#)
- [46] ASTM D1107-96. Standard Test Method for Ethanol-Toluene Solubility of Wood. American Society for Testing and Materials; 1996.
- [47] Kurschner K, Hoffer A. Cellulose and cellulose derivative. *Fresenius J Anal Chem* 1969;92:145-154.
- [48] ASTM D1106-96. Standard Test Method for Acid-Insoluble Lignin in Wood. American Society for Testing and Materials; 1996.
- [49] He Z, Xia Z, Hu J, Ma L, Li Y. Thermal decomposition and kinetics of electrically controlled solid propellant through thermogravimetric analysis. *J Therm Anal Calorim* 2020;139:2187-2195. [\[CrossRef\]](#)
- [50] Merdun H, Boubacar Laougé Z. Kinetic and thermodynamic analyses during co-pyrolysis of greenhouse wastes and coal by TGA. *Renew Energy* 2021;163:453-464. [\[CrossRef\]](#)
- [51] Braga RM, Costa TR, Freitas JCO, Barros JMF, Melo DMA, Melo MAF. Pyrolysis kinetics of elephant grass pretreated biomasses. *J Therm Anal Calorim* 2014;117:1341-1348. [\[CrossRef\]](#)
- [52] Palamanit A, Khongphakdi P, Tirawanichakul Y, Phusunti N. Investigation of yields and qualities of pyrolysis products obtained from oil palm biomass using an agitated bed pyrolysis reactor. *Biofuel Res J* 2019;24:1065-1079. [\[CrossRef\]](#)
- [53] Nemanova V, Abedini A, Lilledahl T, Engvall K. Co-gasification of petroleum coke and biomass. *Fuel* 2014;117:870-875. [\[CrossRef\]](#)
- [54] Özsın G, Pütün AE. Kinetics and evolved gas analysis for pyrolysis of food processing wastes using TGA/MS/FT-IR. *Waste Manag* 2017;64:315-326. [\[CrossRef\]](#)
- [55] Seo MW, Kim S, Lee S, Lee J. Pyrolysis characteristics of coal and RDF blends in non-isothermal and isothermal conditions. *J Anal Appl Pyrolysis* 2010;88:160-167. [\[CrossRef\]](#)

- [56] El May Y, Jeguirim M, Dorge S, Trouvé G, Said R. Study on the thermal behavior of different date palm residues: Characterization and devolatilization kinetics under inert and oxidative atmospheres. *Energy* 2012;44:702-709. [\[CrossRef\]](#)
- [57] Jeguirim M, Tschamber V, Brillhac JF. Kinetics and mechanism of the oxidation of carbon by NO₂ in the presence of water vapor. *Int J Chem Kinet* 2009;41:236-247. [\[CrossRef\]](#)
- [58] Ni Z, Bi H, Jiang C, Wang C, Tian J, Zhou W, et al. Investigation of the co-pyrolysis of coal slime and coffee industry residue based on machine learning methods and TG-FTIR: synergistic effect, kinetics and thermodynamic. *Fuel* 2021;305:121527. [\[CrossRef\]](#)
- [59] Wu Z, Yang W, Tian X, Yang B. Synergistic effects from co-pyrolysis of low-rank coal and model components of microalgae biomass. *Energy Convers Manag* 2017;135:212-225. [\[CrossRef\]](#)
- [60] Jeong HJ, Seo DS, Park SS, Hwang J. A comprehensive study on co-pyrolysis of bituminous coal and pine sawdust using TG. *J Therm Anal Calorim* 2015;120:1867-1875. [\[CrossRef\]](#)
- [61] Yangali P, Celaya AM, Goldfarb JL. Co-pyrolysis reaction rates and activation energies of West Virginia coal and cherry pit blends. *J Anal Appl Pyrolysis* 2014;108:203-211. [\[CrossRef\]](#)
- [62] Gómez-Siurana A, Marcilla A, Beltrán M, Berenguer D, Martínez-Castellanos I, Menargues S. TGA/FTIR study of tobacco and glycerol-tobacco mixtures. *Thermochim Acta* 2013;573:146-157. [\[CrossRef\]](#)
- [63] Berbenni V, Marini A, Bruni G, Zerlia T. TG/FT-IR: an analysis of the conditions affecting the combined TG/spectral response. *Thermochim Acta* 1995;258:125-133. [\[CrossRef\]](#)
- [64] Fang S, Yu Z, Ma X, Lin Y, Lin Y, Chen L, et al. Co-pyrolysis characters between combustible solid waste and paper mill sludge by TG-FTIR and Py-GC/MS. *Energy Convers Manag* 2017;144:114-122. [\[CrossRef\]](#)
- [65] Calabuig E, Juárez-Serrano N, Marcilla A. TG-FTIR study of evolved gas in the decomposition of different types of tobacco. Effect of the addition of SBA-15. *Thermochim Acta* 2019;671:209-219. [\[CrossRef\]](#)
- [66] Orfao J, Antunes FJA, Figueiredo JL. Pyrolysis kinetics of lignocellulosic materials-three independent reactions model. *Fuel* 1999;78:349-358. [\[CrossRef\]](#)
- [67] Blanco López MC, Blanco CG, Martínez-Alonso A, Tascón JMD. Composition of gases released during olive stones pyrolysis. *J Anal Appl Pyrolysis* 2002;65:313-322. [\[CrossRef\]](#)